Class-iF^{-1}: Linearity Enhanced High Efficiency Power Amplifier

Chenhao Chu[1], Sagar K. Dhar[2], Tushar Sharma[3], and Anding Zhu[1]
[1]University College Dublin, Dublin, Ireland
[2]University of Calgary, Alberta, Canada
[3]Indian Institute of Technology Bombay, Mumbai, India
Email: chenhao.chu@ucdconnect.ie

***Abstract*—This paper presents a new class of power amplifier (PA) – Class-iF^{-1} – resolving the highly nonlinear double inflection characteristics in the conventional Class-F^{-1} PA. It is illustrated that, by properly terminating the second harmonic source impedance (Z_{2S}) from conventional short-circuit to open-circuit, the double inflection nonlinear gain profile can be mitigated in the proposed Class-iF^{-1} PA, wherein the same saturation output power is achieved with less gain compression without drain efficiency trade-off. The idea was validated with source/load-pull and a broadband prototype operating from 2.0 to 2.6 GHz was designed using a commercial 10-W Gallium Nitride (GaN) transistor. Under continuous wave (CW) signal test, the proposed Class-iF^{-1} PA can achieve 40.1-40.8-dBm output power, 71.2%-77.3% drain efficiency (DE) and 67.4%-74.1% power added efficiency (PAE) at 3-dB gain compression level over 2.0-2.6 GHz.**

***Index Terms*—5G, Class-F^{-1}, Gallium Nitride (GaN), harmonic tuning, high efficiency, linearity, power amplifier (PA).**

I. Introduction

In the fifth generation (5G) wireless communication systems, the consistent demands of high efficiency and high data rates have imposed significant challenges in radio frequency (RF) power amplifier (PA) design. The Gallium Nitride (GaN)-based RF PAs are gradually used in 5G cellular base stations at sub-6 GHz. Input and output harmonic tuning techniques have been widely used in highly efficient GaN PA designs by manipulating the drain voltage and current waveforms at the intrinsic plane of the active device [1]–[6]. While the Class-F PA has open-circuit second harmonic load (Z_{2L}) termination and short-circuit third harmonic load (Z_{3L}) termination, the Class-F^{-1} PA has the reversed Z_{2L} and Z_{3L} termination condition, achieving excellent theoretical drain efficiency (DE) of ~91% at saturation. However, the nonlinearity performance prevents the Class-F^{-1} PAs from some practical applications, because of the double inflection gain profile [7].

To alleviate the double inflection gain profile of the conventional Class-F^{-1} PA, in this work, we propose a new Class of PA, designated as Class-iF^{-1} PA, by accurately tuning harmonics at the source and properly exploiting the device input nonlinearity. Instead of the short-circuit second harmonic source (Z_{2S}) termination for the conventional Class-F^{-1} PAs, the newly proposed Class-iF^{-1} PA with input harmonic control, enhances the nonlinearity performance by using the open-circuit Z_{2S} termination.

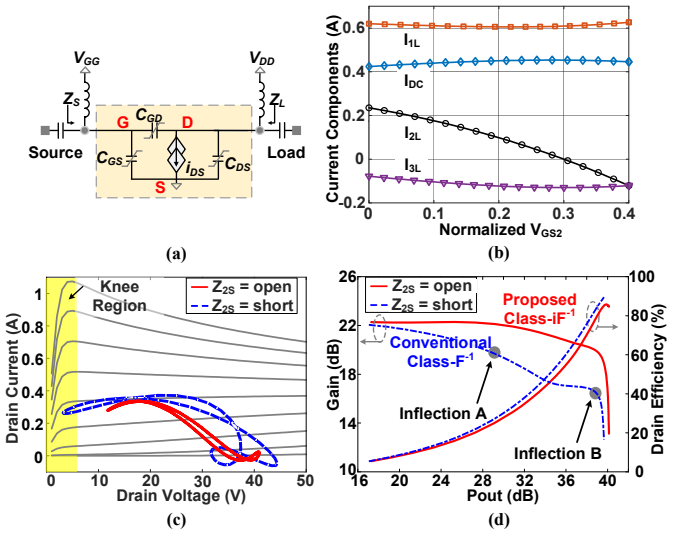

Fig. 1. (a) Simplified GaN device model with input and output nonlinearity; (b) Theoretical drain current components variation with different V_{GS2} (normalized to V_{GS1}); (c) DC-IV curve and loadlines with Z_{2S} open and Z_{2S} short in the low power region; (d) load-pull results for the conventional Class-F^{-1} PA and the proposed Class-iF^{-1}.

II. Proposed Class-iF^{-1} PA

A. Theoretical Modeling Analysis

Fig. 1 (a) shows a simplified GaN device model, wherein the nonlinear C_{GS}-V_{GS} profile generates second harmonic voltage component, leading to the input nonlinearity [5]. The gate voltage waveform can be expressed as

$$v_{GS}(\theta) = V_{GS0} + V_{GS1}\cos\theta - V_{GS2}\cos(2\theta) \quad (1)$$

where V_{GS0} is the DC gate bias voltage, V_{GS1} and V_{GS2} are the fundamental and second harmonic gate voltage components, respectively. In the conventional Class-F^{-1} PA, $V_{GS2} = 0$, meaning the Z_{2S} termination is short-circuit. However, different Z_{2S} terminations other than short can generate out-of-phase V_{GS2} components due to C_{GS} nonlinearity and results in drain current second harmonic component (I_{2L}) variation as shown in Fig. 1 (b).

To understand the Z_{2S} termination impact, the generalized drain voltage waveform can be expressed as

$$v_{DS}(\theta) = V_{DD} - I_{1L}Z_{1L}\cos\theta - I_{2L}Z_{2L}\cos 2\theta - I_{3L}Z_{3L}\cos 3\theta \quad (2)$$

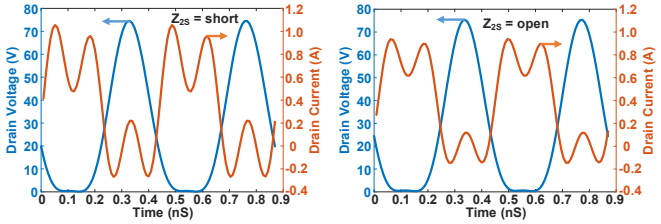

(a) (b)

Fig. 2. Intrinsic drain and current waveforms at saturated output power level (a) Z_{2S} with short termination, (b) Z_{2S} with open termination.

TABLE I
PERFORMANCE COMPARISON BETWEEN CLASS-F^{-1} AND CLASS-IF^{-1} PAS UNDER MODULATED SIGNAL STIMULATION.

Parameters	Conventional Class-F^{-1} PA	Proposed Class-iF^{-1} PA
Pout (dBm)	30	30
ACPR (dBc)	-30.7	-34.1
PAE (%)	36.3	35.2
Gain (dB)	17.1	18.8

where $I_{nL}, Z_{nL}(n = 1, 2, 3)$ denote the fundamental, second and third harmonic drain current components, and impedance terminations, respectively. For the conventional Class-F^{-1} PA, the drain voltage component $I_{2L}Z_{2L}$ in (2) becomes large value because of the high I_{2L} component (as shown in Fig. 1 (b) when $V_{GS2} = 0$) multiplied by open Z_{2L} termination. This causes overall loadline entering into the knee region at the very early input power level as shown in Fig. 1 (c) (blue dotted line). Such knee region operation starting from low power level of the conventional Class-F^{-1} PA leads to the double inflection behavior and makes the gain profile highly nonlinear as shown in Fig. 1 (d) [7]–[9].

This paper exploits input nonlinearity to generate out-of-phase second harmonic gate voltage component V_{GS2}. Fig. 1 (b) clearly shows that the drain current components I_{DC}, I_{1L}, and I_{3L} are almost constant with the variation of V_{GS2}, while the second harmonic drain current component I_{2L} drops as V_{GS2} increases. Thus, the effective I_{2L} component is decreased at the device output and the second harmonic drain voltage component $I_{2L}Z_{2L}$ is significantly reduced. This magnitude control of $I_{2L}Z_{2L}$ helps reducing the drain voltage swing and effectively help avoiding the early knee voltage operation of the conventional Class-F^{-1} PA. This is evident from the loadline plot at early power level (red solid line) in Fig. 1 (c) that the loadline is delayed entering the early knee region operation which flattens the gain profile as shown in Fig. 1 (d). Thus, an innovative PA class of operation designated as Class-iF^{-1} is proposed in this work which improves PA linearity while maintaining efficiency performance.

B. Load-Pull Simulation Analysis

To demonstrate linearity performance under different Z_{2S} terminations, the load-pull simulation was conducted with GaN 2mm device. The simulation was performed at 2.3 GHz

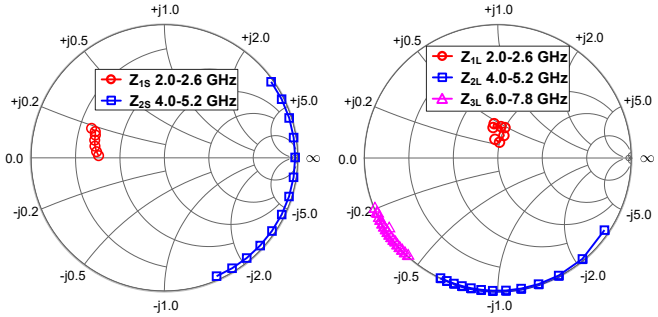

(a) (b)

Fig. 3. Intrinsic trajectories in practical design (a) Source matching network; (b) load matching network.

with controlled load harmonic terminations, second harmonic load impedance Z_{2L} as open, third harmonic load impedance Z_{3L} as short. The fundamental load impedance Z_{1L} was terminated at the maximum efficiency (MXE) point, while the fundamental source termination Z_{1S} was under complex conjugate match.

As presented in Fig. 1 (d), the gain profile has severe double inflection characteristics with Z_{2S} short termination for the conventional Class-F^{-1} PA while the one with Z_{2S} open termination improves gain flatness for the proposed Class-iF^{-1} PA. In terms of the drain efficiency, the Class-iF^{-1} PA with Z_{2S} open termination achieves 85.0% drain efficiency with with 3-dB gain compression compared to the 89.0% DE of the conventional Class-F^{-1} PA with >5-dB gain compression. Fig. 2 shows the intrinsic drain voltage and current waveforms at the same saturated output power level from the load-pull simulation. The voltage waveforms are almost the same for both Z_{2S} short and open cases. While the intrinsic drain current waveforms of Z_{2S} short have larger swing and deeper clipping level compared with that of Z_{2S} open termination.

To further investigate the linearity performance of the proposed Class-iF^{-1} PA, modulated signal simulations were performed. A long-term-evolution (LTE) signal with 8.5-dB peak-to-average-power-ratio (PAPR) is used with GaN 2 mm device with $V_{DD} = 28V$, $V_{GS0} = -3V$. Table I shows the performance comparison with constant output power level. It can be seen that the adjacent channel power ratio (ACPR) was improved by ∼4 dBc with only 1.1% power added efficiency (PAE) trade-off for the proposed Class-iF^{-1} PA. This demonstrates the suitability of the proposed Class-iF^{-1} PA in modern wireless communication systems and proves the improved linearity performance.

III. IMPLEMENTATION AND MEASUREMENTS

A Class-iF^{-1} PA was designed over 2.0-2.6 GHz frequency band with proper source and load terminations as discussed in Section II. A 10-W CG2H40010F transistor from Wolfspeed was used as active device. The simulated intrinsic trajectories over the frequencies are plotted in Fig. 3. It can be seen that the intrinsic second harmonic termination Z_{2S} is over the open-

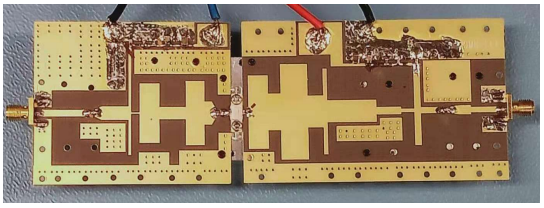

Fig. 4. Photograph of the fabricated Class-iF^{-1} PA.

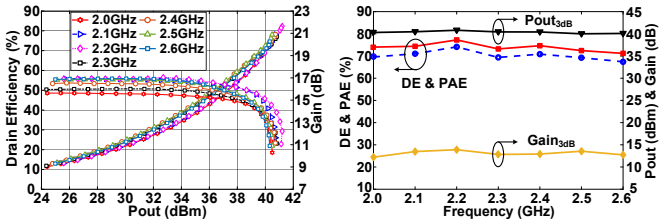

(a) (b)

Fig. 5. Measured results under CW sginal test. (a) DE and gain versus output power; (b) DE, PAE, output power and gain versus frequency over the operation bandwidth.

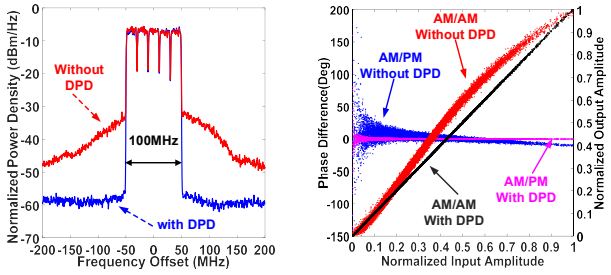

(a) (b)

Fig. 6. Performance with and without DPD linearization of the proposed Class-iF^{-1} PA at 2.3 GHz. (a) Output spectrum; (b) AM–AM and AM–PM.

circuit region in Fig. 3 (a). The intrinsic load trajectories in Fig. 3 (b) indicates the Class-F^{-1} load conditions.

A. Measurement Results with CW Signal

Fig. 4 shows the photograph of the fabricated PA. In the CW signal test, the drain supply voltage was 28 V. Fig. 5 (a) presents the measured drain efficiency, power added efficiency and gain versus output power at different operation frequencies, wherein high saturation efficiency and flat gain response are achieved over the operation bandwidth. The measured DE, PAE, output power and gain at 3-dB gain compression level are presented in Fig. 5 (b). The measurement results show that the proposed Class-iF^{-1} PA can achieve 40.1-40.8-dBm output power, 71.2%-77.3% drain efficiency and 67.4%-74.1% power added efficiency at 3-dB gain compression level over 2.0-2.6 GHz.

B. Measurement Results with Modulated Signal

To evaluate the linearity and efficiency performance of the proposed Class-iF^{-1} PA under modulated signals stimulation, and a 5-carrier 100-MHz LTE signal with 8.5-dB PAPR was used to test the PA. The vector-switch model was applied for digital predistortion (DPD) [10]. The measured adjacent channel power ratios (ACPR)s at 2.3 GHz were -27.23/-25.34 dBc without DPD, and were improved to -50.60/-50.17 dBc with DPD correction as shown in 6 (a).Around 30.74 dBm average output power was achieved after DPD at 2.3 GHz with average DE of 30.68%. The AM-AM and AM-PM characteristics with and without DPD are also given in Fig. 6, showing the well corrected linearity after the DPD performed.

IV. Conclusion

In this paper, we proposed a new class of PA, designated as Class-iF^{-1}. The proposed PA class of operation alleviates the double inflection gain characteristics of the conventional Class-F^{-1} PA. Load-pull simulation results show that the new Class-iF^{-1} PA can provide good output power and high efficiency with less gain compression compared with the conventional Class-F^{-1} PA. To validate the theory, a broadband Class-iF^{-1} PA over 2.0 GHz to 2.6 GHz was designed and fabricated using packaged GaN device. The measurement results show that the proposed Class-iF^{-1} PA can achieve 40.1-40.8-dBm output power, 71.2%-77.3% drain efficiency (DE) and 67.4%-74.1% power added efficiency (PAE) at 3-dB gain compression level over 2.0-2.6 GHz.

References

[1] P. White, "Effect of input harmonic terminations on high efficiency class-B and class-F operation of PHEMT devices," in *IEEE MTT-S Int. Microw. Symp. Dig.*, vol. 3, 1998, pp. 1611–1614.

[2] P. Colantonio, F. Giannini, G. Leuzzi, and E. Limiti., "High efficiency low-voltage power amplifier design by second-harmonic manipulation," *Int. J. RF Microw. Comput.-Aided Eng.*, vol. 10, no. 1, pp. 19–32, Jan. 2000.

[3] T. Canning, P. Tasker, and S. Cripps, "Waveform evidence of gate harmonic short circuit benefits for high efficiency X-band power amplifiers," *IEEE Microw. Wirel. Compon. Lett.*, vol. 23, no. 8, pp. 439–441, 2013.

[4] S. K. Dhar, T. Sharma, N. Zhu, D. Holmes, R. Darraji, and F. M. Ghannouchi, "Comprehensive analysis of input waveform shaping for efficiency enhancement in class-B power amplifiers," in *IEEE MTT-S Int. Microw. Symp. Dig.*, Jun. 2019, pp. 1164–1167.

[5] S. K. Dhar, T. Sharma, R. Darraji, D. G. Holmes, S. V. Illath, V. Mallette, and F. M. Ghannouchi, "Investigation of input–output waveform engineered continuous inverse class F power amplifiers," *IEEE Trans. Microw. Theory Techn.*, vol. 67, no. 9, pp. 3547–3561, Sep. 2019.

[6] S. K. Dhar, T. Sharma, N. Zhu, R. Darraji, D. G. Holmes, J. Staudinger, M. Helaoui, V. Mallette, and F. M. Ghannouchi, "Modeling of input nonlinearity and waveform engineered high-efficiency class-F power amplifiers," *IEEE Trans. Microw. Theory Techn.*, vol. 68, no. 10, pp. 4216–4228, Oct. 2020.

[7] T. Sharma, J. Roberts, D. G. Holmes, R. Darraji, J. K. Jones, and F. M. Ghannouchi, "On the double-inflection characteristic of the continuous-wave am/am in class-F^{-1} power amplifiers," *IEEE Microw. Wirel. Compon. Lett.*, vol. 28, no. 12, pp. 1131–1133, Dec. 2018.

[8] S. K. Dhar, T. Sharma, R. Darraji, D. G. Holmes, J. Staudinger, X. Y. Zhou, V. Mallette, and F. M. Ghannouchi, "Impact of input nonlinearity on efficiency, power, and linearity performance of GaN RF power amplifiers," in *IEEE MTT-S Int. Microw. Symp. Dig.*, Aug. 2020, pp. 281–284.

[9] T. Sharma, J. S. Roberts, S. K. Dhar, S. Shukla, R. Darraji, D. G. Holmes, and F. M. Ghannouchi, "On the efficiency and am/am flatness of inverse class-F power amplifiers," in *IEEE MTT-S Int. Microw. Symp. Dig.*, Jun. 2019, pp. 460–463.

[10] S. Afsardoost, T. Eriksson, and C. Fager, "Digital predistortion using a vector-switched model," *IEEE Trans. Microw. Theory Techn.*, vol. 60, no. 4, pp. 1166–1174, 2012.